PHYSICAL REVIEW B VOLUME 42, NUMBER 10 1 OCTOBER 1990

# Spin dynamics of the itinerant helimagnet MnSi studied by positive muon spin relaxation

R. Kadono*
*Meson Science Laboratory, Faculty of Science, University of Tokyo, 7-3-1 Hongo, Bunkyo-ku, Tokyo 113, Japan*

T. Matsuzaki
*Metal Physics Laboratory, Institute of Physical and Chemical Research, 2-1 Hirosawa, Wako, Saitama 351-01, Japan*

T. Yamazaki
*Institute for Nuclear Study, University of Tokyo, 3-2-1 Midori-cho, Tanashi, Tokyo 188, Japan*

S. R. Kreitzman
*TRIUMF, University at British Columbia, 4004 Wesbrook Mall, Vancouver, British Columbia, Canada V6T2A3*

J. H. Brewer
*Department of Physics, University of British Columbia, Vancouver, British Columbia, Canada V6T2A6*
(Received 2 April 1990)

The local magnetic fields and spin dynamics of the itinerant helimagnet MnSi ($T_c \simeq 29.5$ K) have been studied experimentally using positive muon spin rotation and relaxation ($\mu^+$SR) methods. In the ordered phase ($T < T_c$), zero-field $\mu$SR was used to measure the hyperfine fields at the muon sites as well as the muon spin-lattice relaxation time $T_1^\mu$. Two magnetically inequivalent interstitial $\mu^+$ sites were found with hyperfine coupling constants $A_{\rm hf}^{(1)} = -3.94$ kOe/$\mu_B$ and $A_{\rm hf}^{(2)} = -6.94$ kOe/$\mu_B$, respectively. In the paramagnetic phase ($T > T_c$), the muon–nuclear-spin double-relaxation technique was used to simultaneously but independently determine the spin-lattice relaxation time $T_1^{\rm Mn}$ of $^{55}$Mn spins and that of positive muons ($T_1^\mu$) over a wide temperature range ($T_c < T \leq 150$ K). The temperature dependence of $T_1^{\rm Mn}$ and $T_1^\mu$ in both phases shows systematic deviations from the predictions of self-consistent renormalization theory.

## I. INTRODUCTION

It is well established by neutron-scattering and nuclear-magnetic-resonance (NMR) experiments that manganese monosilicite (MnSi) is a typical itinerant magnet that shows a helical magnetic order with a long period of 180+3 Å ($Q = 0.035$ Å$^{-1}$) below $T_c = 29.5$ K.[1,2] In an external magnetic field, the structure becomes progressively more conical, until above $H_c = 6.2$ kOe (at 4.2 K) it becomes ferromagnetic. The uniform susceptibility above $T_c$ is known to show a Curie-Weiss paramagnetic behavior. Despite such behavior, experiments have shown that various magnetic properties are better explained in terms of the itinerant electron picture rather than the usual localized moment picture.

It is very useful for the understanding of itinerant magnets to study the electronic spin fluctuations which dominate all their thermodynamic properties. The spin-lattice relaxation time ($T_1$) of nuclei or interstitial muons is a good measure of such fluctuations near $T_c$. There have been several experimental investigations of $T_1$ using $^{55}$Mn and $^{29}$Si NMR (Ref. 3) and muon spin-rotation and -relaxation ($\mu$SR) techniques.[4–6] The $\mu$SR study provided unique information on $T_1$ in a wide temperature range including the critical region which was not accessible to the NMR studies.

In the case of $\mu$SR the muon spin polarization is sensitive to both the hyperfine fields of the electrons at the $\mu^+$ and the nuclear dipolar fields of manganese nuclear moments, which in turn are relaxed in a time $T_1^{\rm Mn}$ (the spin-lattice relaxation time of the $^{55}$Mn nuclei) by their own electronic hyperfine fields. All hyperfine fields arise from the same itinerant electrons and therefore fluctuate at the same rate, if at all. The "direct" $\mu^+$ spin-lattice relaxation time $T_1^\mu$ is a measure of this fluctuation rate, as is $T_1^{\rm Mn}$, which manifests itself indirectly in the "motional averaging" of the $\mu^+$ relaxation caused by the nuclear moments. In earlier experiments, Hayano *et al.*[4] measured the temperature dependence of $T_1^\mu$ above $T_c$ (paramagnetic phase) between 29.7 and 36.2 K by applying a longitudinal magnetic field (LF) of $\sim$700 G to decouple the nuclear dipole fields from Mn moments; they found good agreement with theoretical predictions based on the self-consistent renormalization (SCR) theory of spin fluctuations[7] within the measured temperature region. However, in a recent zero-field (ZF) $\mu$SR experiment designed to determine $T_1^{\rm Mn}$ in the $10^{-6}$ s$^{-1}$ range through muon-nuclear double relaxation,[5] the value of $T_c$ extrapolated from the $T$ dependence of $T_1^{\rm Mn}$ using the SCR theory did not agree with the accepted value of $T_c = 29.5$ K; this discrepancy remains to be understood.

In the ordered phase it is known that $T^\mu$ shows a deviation from the theoretical prediction around $|T - T_c| \leq 10$ K,[6] and that the observed hyperfine coupling constant $A_{\rm hf}$ is 17% smaller than that expected from frequency shift measurements in the paramagnetic phase.

Thus, despite experimental and theoretical efforts, we still lack a satisfactory understanding of the itinerant magnet. In order to further explore the magnetic properties of MnSi, we have performed a systematic study of $T_1$ by ZF $\mu$SR below $T_c$ and by ZF and longitudinal field (LF) $\mu$SR above $T_c$. As will be mentioned below, the present work benefits from (i) a muon-beam quality dramatically improved, since most of the previous work,[4,5] allowing measurements of relaxation times as long as $10^{-5}$ s over a wider temperature range than previously possible, and (ii) precise ($\pm 0.02$ K) control of the sample temperature, which is indispensible for measurements close to $T_c$.

## II. MUON SPIN RELAXATION FUNCTION

In a time-differential $\mu$SR experiment, muons are stopped one at a time in the sample, where they decay, emitting positrons preferentially along their final spin polarization $\mathbf{P}_\mu(t)$. Each incoming $\mu^+$ passes through a thin plastic scintillation counter that generates a fast timing pulse that starts a time digitizer ("clock"). For ZF or LF $\mu$SR experiments, two thick scintillators are placed parallel (+) and antiparallel (−) to the initial muon spin polarization $\mathbf{P}_\mu(0)=\hat{\mathbf{z}}$; a decay positron passing through either of these detectors stops the "clock," whereupon the digitized time interval is binned in the corresponding time histogram, which has the form

$$N_\pm(t)=\mathcal{N}_0^\pm e^{-t/\tau_\mu}[1\pm A_\pm P_z^\mu(t)]+B_\pm \ , \quad (1)$$

where $\tau_\mu$ is the muon decay lifetime, $A_\pm$ is the spatial anisotropy or "asymmetry" (typically 0.2–0.3) for the corresponding $e^+$ detector, $P_z^\mu(t)\equiv\hat{\mathbf{z}}\cdot\mathbf{P}_\mu(t)$ is the longitudinal muon spin polarization, and $B_\pm$ is a time-independent background. In cases where the spin polarization relaxes to zero within the observable time range, $P_z^\mu(t)$ can be determined redundantly by fitting both time spectra independently to Eq. (1). More often, the information contained in the two spectra must be combined. The backgrounds $B_\pm$ are evaluated from the $t<0$ region of each spectrum and subtracted from $N_\pm(t)$ to get $\mathcal{N}_\pm(t)\equiv N_\pm(t)-B_\pm$, from which one constructs the empirical "raw" asymmetry $\mathcal{R}_z(t)$:

$$\mathcal{R}_z(t)\equiv\frac{\mathcal{N}_+(t)-\mathcal{N}_-(t)}{\mathcal{N}_+(t)+\mathcal{N}_-(t)} \ , \quad (2)$$

which can be converted to the "corrected" asymmetry

$$\mathcal{A}_z(t)=\frac{(1+\alpha)\mathcal{R}_z(t)-(1-\alpha)}{(1+\alpha\beta)-(1-\alpha\beta)\mathcal{R}_z(t)}=A_+P_z^\mu(t) \ , \quad (3)$$

where $\alpha\equiv\mathcal{N}_0^-/\mathcal{N}_0^+$ is a correction factor coming from the different efficiencies of the two detectors and $\beta\equiv A_-/A_+\approx 1$ is a similar factor accounting for their different intrinsic asymmetries. Note that for $\alpha=\beta=1$, $\mathcal{A}_z(t)=\mathcal{R}_z(t)$. The raw asymmetry spectrum $\mathcal{R}_z(t)$ derived from the data as described in Eq. (2) is actually fitted to

$$\mathcal{R}_z(t)=\frac{(1+\alpha\beta)A_+P_z^\mu(t)+(1-\alpha)}{(1+\alpha)+(1-\alpha\beta)A_+P_z^\mu(t)} \ , \quad (4)$$

with $\alpha$, $\beta$, $A_+$, and the theoretical variables defining $P_z^\mu(t)$ as fitted parameters. [In most cases $\beta$ is so close to unity that $\beta=1$ is assumed in the fits; otherwise $\beta$ is determined independently from transversely applied magnetic field (TF) $\mu$SR measurements in the same geometry and then held fixed.]

### A. Ordered phase

In the ordered phase of a randomly oriented multidomain sample (assuming that the muons occupy a unique crystallographic site), the longitudinal muon spin polarization $P_z^\mu(t)$ has the form[6]

$$P_z^\mu(t)=\tfrac{1}{3}e^{-t/T_1^\mu}+\tfrac{2}{3}e^{-t/T_2}\cos\omega t \ , \quad (5)$$

where $T_2$ is the transverse spin relaxation time and $\omega=\gamma_\mu H_{\rm loc}$ ($\gamma_\mu=2\pi\times 13.55$ kHz/Oe is the muon gyromagnetic ratio) is the muon angular frequency determined by the local magnetic-field magnitude $H_{\rm loc}$. The transverse relaxation is caused by a combination of temporal fluctuations in the direction of $\mathbf{H}_{\rm loc}$ and static spatial inhomogeneities in its magnitude $H_{\rm loc}$. Because of the strong local field due to the itinerant electrons, the effect of $^{55}$Mn nuclear moments (whether static or fluctuating) is insignificant for the $\frac{1}{3}$ component in which $\mathbf{H}_{\rm loc}$ is initially parallel to $\mathbf{P}_\mu(0)=\hat{\mathbf{z}}$. For this component, then, the relaxation rate $1/T_1^\mu$ is a function only of the fluctuations of $\mathbf{H}_{\rm loc}$ in time.

There are two familiar limiting cases for $T_1^\mu$: In the first, called the "'static limit," $1/T_1^\mu$ is simply the rate at which the direction of $\mathbf{H}_{\rm loc}$ fluctuates so as to introduce new (large) transverse components; on average, $\frac{1}{3}$ of the new field components will still be along $\hat{\mathbf{z}}$, leaving $1/T_1^\mu=\frac{2}{3}(1/\tau_c)$ or $T_1^\mu=\frac{3}{2}\tau_c$, where $\tau_c$ is the correlation time of the local field.[8,9] In the second limit, called the "fast-fluctuation limit," $\mathbf{H}_{\rm loc}$ is fluctuating very fast, but has a nonzero mean value $\langle\mathbf{H}_{\rm loc}\rangle$ that represents the "static" local field detected via the coherent $\mu^+$ precession signal; the remaining (fluctuating) components have a magnitude $\omega_0/\gamma_\mu$ and produce a spin-lattice relaxation rate $1/T_1^\mu\approx\omega_0^2\tau_c$.[10]

If (as is the case in MnSi—see below) there are two magnetically inequivalent muon sites with populations $p_1$ and $p_2$ (with $p_1+p_2=1$), then Eq. (5) becomes

$$P_z^\mu(t)=p_1(\tfrac{1}{3}e^{-t/T_1^{(1)}}+\tfrac{2}{3}e^{-t/T_2^{(1)}}\cos\omega_1 t)+p_2(\tfrac{1}{3}e^{-t/T_1^{(2)}}+\tfrac{2}{3}e^{-t/T_2^{(2)}}\cos\omega_2 t) \ . \quad (6)$$

### B. Paramagnetic phase

In situations where the time evolution of the muon spin polarization is best characterized as "relaxation," as opposed to the coherent precession seen in TF or the oscillatory polarization seen in magnetically ordered phases, it is conventional[8] to describe $P_z^\mu(t)$ in terms of a longitudinal spin-relaxation function

$$G_{zz}(t) \equiv \langle \mathbf{P}_\mu(t) \cdot \mathbf{P}_\mu(0) \rangle / |\mathbf{P}_\mu(0)|^2 .$$

The spin relaxation of muons in the paramagnetic phase of MnSi can be described approximately[5] by the product of two relaxation functions from two independent sources, one due to rapidly fluctuating itinerant electrons and the other due to nuclear dipolar fields:

$$G_{zz}(t) = e^{-t/T_1^\mu} G_{zz}^{\mathrm{KT}}(t; T_1^{\mathrm{Mn}}) , \quad (7)$$

where $G_{zz}^{\mathrm{KT}}(t; T_1^{\mathrm{Mn}})$ is the dynamical Kubo-Toyabe relaxation function[8] involving $T_1^{\mathrm{Mn}}$ as the correlation time of the nuclear dipolar field. In this way the so-called muon–nuclear-spin double-relaxation function[5] is capable of determining not only $T_1^\mu$ but also $T_1^{\mathrm{Mn}}$. Since the muon is evidently self-trapped in MnSi below room temperature as implied in the earlier experiments,[5,6] the correlation time due to $\mu^+$ motion need not be considered. In the static limit ($T_1^{\mathrm{Mn}} \to \infty$), the Kubo-Toyabe function is written analytically as

$$g_{zz}^{\mathrm{KT}}(t) \equiv G_{zz}^{\mathrm{KT}}(t; \infty) = \tfrac{1}{3} + \tfrac{2}{3}(1 - \Delta^2 t^2) e^{-\Delta^2 t^2 / 2} , \quad (8)$$

where $\Delta/\gamma_\mu$ is the rms value of the Gaussian distribution of static nuclear dipolar fields: $\Delta^2/\gamma_\mu^2 \equiv \langle H_x^2 \rangle = \langle H_y^2 \rangle = \langle H_z^2 \rangle$.

Since the local field Mn moments is small ($\Delta/\gamma_\mu \sim 5$ Oe) and that from the itinerant electrons is large (see below), by applying a magnetic field of 100–200 Oe we can quench the nuclear part of the relaxation [i.e., $G_{zz}^{\mathrm{KT}}(t; T_1^{\mathrm{Mn}}) \to 1$] without significantly affecting the electronic part [$\exp(-t/T_1^{\mathrm{Mn}})$] and thus obtain an independent measurement of $T_1^\mu$. [This presupposes that the LF chosen does not produce an accidental degeneracy between the $^{55}$Mn nuclear quadrupolar splitting and the $\mu^+$ Zeeman splitting; such a degeneracy can produce a "level-crossing resonance" (LCR) in the muon relaxation rate[11] and confound the experimental results.] In the present experiment we measured $\mu$SR spectra for both ZF and LF ($\sim 120$ Oe) at every temperature.

Again, the situation may be more complicated in the case where muons at two different sites see different hyperfine fields. All $^{55}$Mn nuclei presumably see the same $T_1^{\mathrm{Mn}}$, and all muon sites presumably see the same nuclear dipolar fields, so both sites should share the same $G_{zz}^{\mathrm{KT}}(t; T_1^{\mathrm{Mn}})$ factor, but will have different values of $T_1^\mu$ as in the ordered phase

$$G_{zz}(t) = G_{zz}^{\mathrm{KT}}(t; T_1^{\mathrm{Mn}})(p_1 e^{-t/T_1^{(1)}} + p_2 e^{-t/T_1^{(2)}}) . \quad (9)$$

## III. EXPERIMENT

This experiment was conducted at the M9 muon channel of TRIUMF using an electrostatic "Wien filter" (velocity selector) as a muon-positron particle separator. A 100% spin-polarized "surface muon" beam (momentum $\approx 28$ MeV/$c$) was stopped in a single-crystal sample of MnSi inside a helium gas flow cryostat, and the decay positron time spectra were measured in the range 0–10 $\mu$s with a conventional $\mu$SR experimental apparatus.[12] To achieve precise control of the sample temperature, two-stage temperature regulation was introduced: The temperature of the helium gas diffuser (and thus of the He gas flowing past the sample container) was regulated at a temperature just below the desired sample temperature $T_{\mathrm{meas}}$, while that of the copper cell containing the sample was regulated independently at $T_{\mathrm{meas}}$. Using this system, the sample temperature was controlled to within 0.02 K near $T_c$.

The data were analyzed by $\chi^2$-minimization fitting of the raw asymmetry spectrum [Eq. (2)] to the form of Eq. (4) using the appropriate time dependence of $P_z^\mu$, i.e., Eqs. (7) or (9) for the paramagnetic phase and Eq. (6) for the ordered phase.

## IV. RESULTS

### A. Ordered phase

Several typical $\mu$SR time spectra for $T < T_c$ are shown in the range $0 < t < 1$ $\mu$s in Fig. 1. Two different frequency components can be clearly identified in these spectra; this feature was obscured in the earlier experiment, presumably due to the limited statistical accuracy and considerable backgrounds. The two frequencies correspond to two magnetically inequivalent sites for muons in MnSi. This could be explained by the rather complicated crystal structure of MnSi (B20 cubic symmetry).

The results of the $\chi^2$-minimization fitting analysis are shown in Table I. In order to obtain good fits to Eq. (6), we assumed $1/T_1^{(i)} = \theta(f^{(i)})^2$, where $f^{(i)} \equiv \omega^{(i)}/2\pi$ and $\theta$ is an effective correlation time common to both sites. If the *static limit* is applied in the ordered state, one would ex-

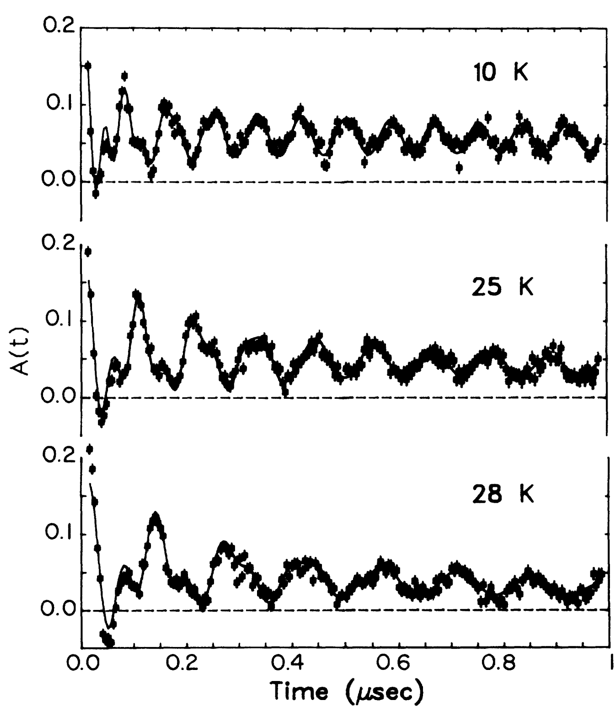


FIG. 1. Corrected muon-decay position asymmetry time spectra $\mathcal{A}(t) = A_+ P_z^\mu(t)$ from muons in MnSi at 10, 25, and 28 K. The solid lines indicate the best fits to a function with two local field components (see text).

TABLE I. Muon spin precession frequency ($f^{(i)}$) and local field correlation time [$\theta \equiv 1/T_1^{(i)}(f^{(i)})^2$] in MnSi below $T_c$. The corresponding spin-lattice relaxation time $T_1^{(i)}$ is fitted as $1/T_1^{(i)} = \theta(f^{(i)})^2$ $(i=1,2)$.

| Temperature (K) | $f^{(1)}$ (MHz) | $f^{(2)}$ (MHz) | $\theta$ ($\mu$s) |
|---|---|---|---|
| 6.00(2) | 12.249(6) | 28.07(7) | $0.19(1)\times 10^{-3}$ |
| 10.00(2) | 11.930(5) | 27.30(7) | $0.31(1)\times 10^{-3}$ |
| 15.50(2) | 11.266(6) | 25.83(6) | $0.59(4)\times 10^{-3}$ |
| 20.00(5) | 10.447(8) | 23.73(4) | $0.75(8)\times 10^{-3}$ |
| 25.00(5) | 8.957(5) | 20.40(2) | $1.68(3)\times 10^{-3}$ |
| 26.00(5) | 8.48(1) | 19.40(2) | $2.20(6)\times 10^{-3}$ |
| 27.00(2) | 7.85(1) | 18.03(5) | $2.73(8)\times 10^{-3}$ |
| 28.00(2) | 7.024(6) | 16.10(1) | $5.70(9)\times 10^{-3}$ |
| 29.00(2) | 5.52(3) | 12.56(5) | $4.61(12)\times 10^{-2}$ |
| 29.30(2) | 4.73(15) | 11.38(78) | $4.21(46)\times 10^{-2}$ |

pect $T_1^{(1)} = T_1^{(2)} = T_1^{\mu}$ and $1/T_2^{(i)} = 1/T_1^{\mu} + \xi\omega_i$, where the dimensionless constant $\xi$ (representing the *fractional* inhomogeneity of the local field) should be same for both sites. In fact, this seems not to be the case; instead, we find that $1/T_2^{(i)} - 1/T_1^{(i)}$ scales approximately as $\omega_i^2$ (the *square* of $\gamma_\mu$ times the local field strength), as expected in the *fast-fluctuating limit*. The same should then be true of $T_1^{(i)}$, but the data are not sufficiently precise to reveal two separate longitudinal relaxation rates, hence the empirical treatment described above.

The local field $H_{\rm loc}$ felt by the muon satisfies

$$H_{\rm hf}(T) = H_{\rm loc}(T) - \frac{4\pi}{3} M_Q(T) , \tag{10}$$

$$H_{\rm hf}(T) = A_{\rm hf} M_Q(T) , \tag{11}$$

where $H_{\rm hf}$ is the hyperfine field, $M_Q$ is the saturation magnetization, and $A_{\rm hf}$ is the muon's hyperfine coupling constant. Using the known value of $M_Q(0) = 0.39\mu_b/\text{Mn}$ and that $A_{\rm hf}$ is negative and temperature independent,[6] we can deduce $A_{\rm hf}^{(i)}$ from the observed muon precession frequencies $\omega_i$ at 6.0 K:

$$A_{\rm hf}^{(1)} = -3.94 \text{ kOe}/\mu_B , \tag{12}$$

and

$$A_{\rm hf}^{(2)} = -6.94 \text{ kOe}/\mu_B . \tag{13}$$

Figure 2 shows the local magnetic field at the $\mu^+$ as a function of temperature, including the data of Ref. 6, which correspond to the smaller component of $H_{\rm loc}$ ($A_{\rm hf}^{(1)} = -3.94$ kOe/$\mu_B$). The agreement between the temperature dependence of $H_{\rm loc}$ and that of $M_Q(T)$ as determined by neutron scattering[13] (dashed curves in Fig. 2) indicates that the relationship $H_{\rm loc} \propto M_Q(T)$ is well satisfied. The ratio of populations $p_1/p_2$ is $0.77 \pm 0.09$, almost independent of temperature from 6 to 29 K. The weighted average of the hyperfine coupling constant is

$$\overline{A}_{\rm hf} = p_1 A_{\rm hf}^{(1)} + p_2 A_{\rm hf}^{(2)} = -5.63 \text{ kOe}/\mu_B , \tag{14}$$

the magnitude of which is 17% *larger* than that of the value $-4.8$ kOe/$\mu_B$ deduced from the Knight shift versus susceptibility plot in the paramagnetic phase.[14] The curve predicted by SCR theory for the magnetization $M_Q(T)$ is plotted in Fig. 2 for comparison, showing the same disagreement between the experimental shape of $H_{\rm loc}(T)$ and the theoretical shape of $M_Q(T)$ as observed in the previous experiment.[6]

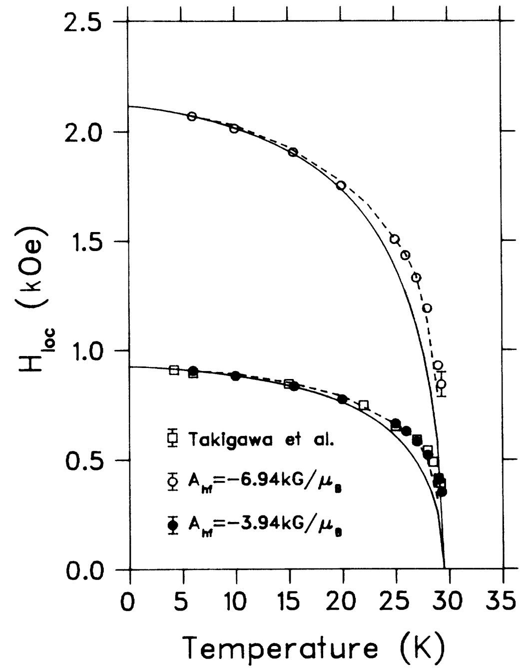


FIG. 2. Temperature dependence of the local magnetic fields $H_{\rm loc}$ felt by muons. Previous data are shown as open squares. Solid lines: theoretical calculation of the normalized magnetization $M_Q(T)/M_Q(0)$. Dashed lines: $M_Q(T)/M_Q(0)$ determined from neutron scattering.

The muon spin-lattice relaxation time $T_1^{\mu}$ is determined by the dynamical fluctuation of the hyperfine field at the muon site. Figure 3 shows a plot of $1/T_1^{(1)} = (f^{(1)})^2\theta$ and $1/T_2^{(2)} = (f^{(2)})^2\theta$ versus temperature. Since we assumed that $\theta$ is common to both $T_1^{(i)}$, the fitted value of $1/T_1^{(2)}$ is automatically a factor of $(f^{(2)})^2/(f^{(1)})^2$ larger than that of $1/T_1^{(1)}$. Therefore, we disregard the distinction between them hereafter.

According to the SCR theory, both spin-lattice relaxation rates should obey

$$1/T_1 \propto T/[M_Q(T)]^2 , \tag{15}$$

below $T_c$.[7] Figure 4 shows a plot of $f_i^2/T_1^{(i)}$ versus $T$, which is expected to be linear if Eq. (15) is satisfied. Here also we observe a trend of deviation from the SCR theory: $f_i^2/T_1^{(i)}$ is almost linear in $T$ below 20 K but falls below this line above 20 K. The best linear fit to the data below 20 K gives

$$\frac{1}{T_1^{(1)}} = 4.03(1)\times 10^{-3} \frac{T}{m^2} , \tag{16}$$

and

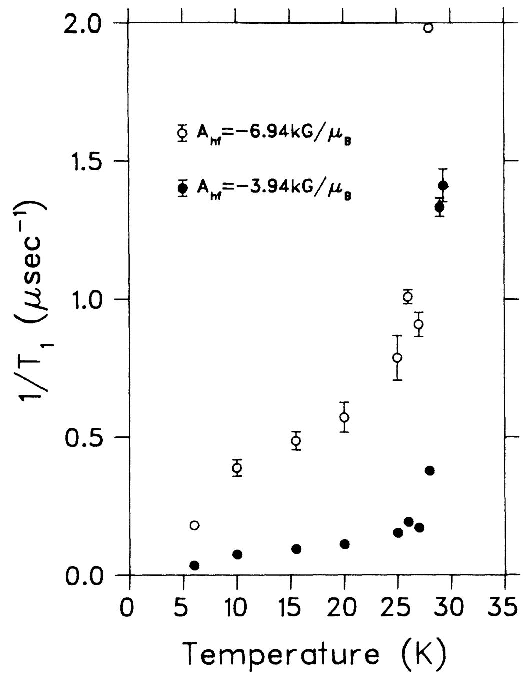


FIG. 3. Spin-lattice relaxation rates $1/T_1$ vs temperature in the ordered phase of MnSi.

$$\frac{1}{T_1^{(2)}}=2.1(1)\times10^{-2}\frac{T}{m^2}\ , \tag{17}$$

with $T_1^{(1)}$ and $T_1^{(2)}$ in $\mu$s and $T$ in K, and where $m\equiv M_Q(T)/M_Q(0)$. The mean value of these two is consistent with the previous experimental result.

The authors of Ref. 6 offer an interpretation of the deviation of $1/T_1$ from $T/m^2$ in terms of the weak antiferromagnetic behavior of the helically ordered state. They claim that since the spin fluctuation in a small region around $Q$ plays an important role near $T_c$, the SCR theory for the weak *antiferromagnetic* metals[15] might be more effective in describing $1/T_1$.[16,17] That theory predicts $1/T_1\propto T/M_Q(T)$, which would explain the general behavior of the temperature dependence for 20 $\mathrm{K}\leq T\leq T_c$.

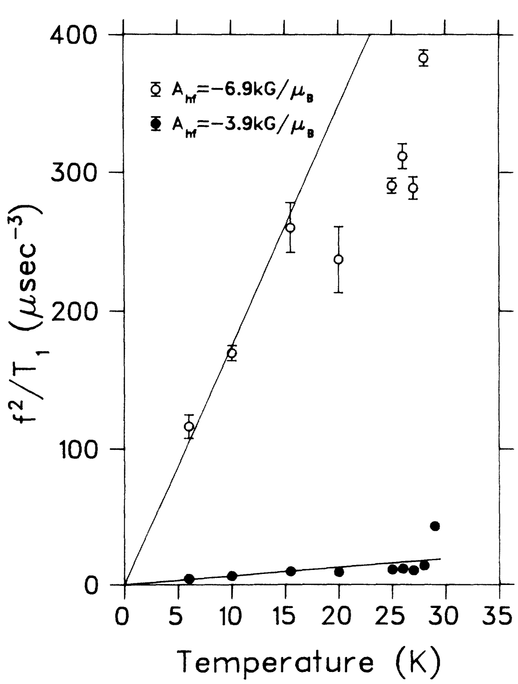


FIG. 4. Plot of $f^2/T_1$ vs temperature. Solid lines show the fit to a linear function below 20 K.

### B. Paramagnetic phase

The ZF and LF $\mu$SR time spectra at each temperature were analyzed simultaneously with common values of $\alpha$, $\beta$, $A_+$, and $T_1^{\mu}$. This helped to eliminate ambiguities due to very long $T_1^{\mu}$ relaxation times at high $T$ and very short $T_1^{\mathrm{Mn}}$ near $T_c$. However, the subtleties of fitting the product of two relaxation functions introduced other uncertainties, as will be discussed below.

In a preliminary analysis we found that the background $B$ for one of the two positron detectors was three times higher ($\sim$3.6%) than that for the other detector. This means that the signal-to-noise ratio in that detector's time histogram becomes equal to unity around

$$t_e=-\tau_\mu \ln(0.036)\simeq 7\ \mu\text{s}\ ,$$

beyond which time the spectrum is dominated by background. To avoid systematic errors due to this background for $T_1$ (especially $T_1^{\mathrm{Mn}}$) larger than $t_e$, we used only the signal of the lower-background detector for the final analysis.

Examples of the spectra at typical temperatures are shown in Fig. 5 with the best-fit curves using Eq. (7). As can be seen, the time spectra in this phase show drastic changes as the spin-lattice relaxation times $T_1^{\mu}$ and $T_1^{\mathrm{Mn}}$ change with temperature. The deduced values for $T_1^{\mu}$, $T_1^{\mathrm{Mn}}$, and the static dipolar width $\Delta$ at each temperature are shown in Table II.

The same data were compared with Eq. (9) using a ratio $p_1/p_2$ fixed by the ordered-phase analysis. Close to $T_c$ a better fit is indeed obtained using different values of $T_1^{(1)}$ and $T_1^{(2)}$; however, within a few K of $T_c$ this analysis produced identical values of $T_1^{(1)}$ and $T_1^{(2)}$. Moreover, where $T_1^{(1)}$ and $T_1^{(2)}$ are different, their ratio is not that predicted by SCR theory. Since the fitted $T$ dependence of $T_1^{(1)}$ and $T_1^{(2)}$ (where they differ) follows that of $T_1^{\mu}$ in the fits to Eq. (7), and, since we have no explanation for the observed behavior (see, however, the conjectures below), we have limited our final analysis to a single $T_1^{\mu}$ [i.e., Eq. (7)—which, as can be seen from Fig. 5, gives a quite adequate fit to the data in most cases.

The spin-lattice relaxation times $T_1^{\mu}$ and $T_1^{\mathrm{Mn}}$ are plotted as $1/T_1$ versus $T-T_c$ (assuming $T_c$=29.5 K) in Fig. 6. The $T$ dependence shows a kink around $T-T_c\simeq10$ K for both $T_1^{\mu}$ and $T_1^{\mathrm{Mn}}$. Assuming that the curve is described by $1/T_1\propto1/(T-T_c)^{\beta}$, the exponent $\beta$ is estimated to be $\approx1.5$ for $1\leq T-T_c\leq10$ K; the $T$ dependences of $T_1^{\mu}$ and $T_1^{\mathrm{Mn}}$ seem to scale in this temperature region. For $T-T_c\geq10$ K, on the other hand, both $T_1^{\mu}$ and $T_1^{\mathrm{Mn}}$ show much weaker $T$ dependence ($\beta\leq0.5$).

It is interesting to note that this weak $T$ dependence resembles that in the weak antiferromagnetic itinerant magnets above $T_c$, i.e., $1/T_1 \propto T/\sqrt{T-T_c}$.[15] For $T-T_c \leq 0.5$ K, fits to the time spectra using a simple exponential relaxation function give poor $\chi^2$ values, suggesting that the fitted values of $T_1^\mu$ are less reliable in this region. This might be due to an onset of "critical divergence" near $T_c$.

Figure 7 shows $T_1^\mu$ and $T_1^{\mathrm{Mn}}$ plotted versus $1/T$ along with data from Ref. 5. In this graph the prediction of the SCR theory that $1/T_1 \propto T(T-T_c)$ (Ref. 7) corresponds to a linear function. The present data do not show a linear dependence near $T_c$. The discrepancy of $T_c$ claimed in Ref. 5 can be partly attributed to the arbitrary choice of the temperature region used for the extrapolation. At high temperatures $T_1^\mu$ shows a considerable deviation from that extrapolated from the vicinity of $T_c$ using the SCR theory. This is evident from inspection of the LF $\mu$SR spectra, which exhibit unmistakable relaxation even at 150 K.

The ratio of $T_1^\mu$ to $T_1^{\mathrm{Mn}}$ is plotted as a function of

TABLE II. Static dipolar width $\Delta$ and spin-lattice relaxation times $T_1^\mu$ and $T_1^{\mathrm{Mn}}$ in paramagnetic MnSi.

| Temperature (K) | $\Delta$ ($\mu s^{-1}$) | $1/T_1^\mu$ ($\mu s^{-1}$) | $1/T_1^{\mathrm{Mn}}$ ($\mu s^{-1}$) |
|---|---|---|---|
| 150.0(1) | 0.324(1) | 0.0233(6) | <0.001 |
| 120.0(1) | 0.316(1) | 0.0272(6) | 0.002(5) |
| 101.00(5) | 0.313(1) | 0.0273(7) | <0.001 |
| 65.00(4) | 0.310(1) | 0.0356(5) | 0.067(5) |
| 46.00(4) | 0.284(1) | 0.0555(6) | 0.076(6) |
| 38.00(4) | 0.279(1) | 0.0733(7) | 0.118(7) |
| 36.00(2) | 0.277(1) | 0.0723(6) | 0.197(7) |
| 34.00(2) | 0.275(2) | 0.0849(8) | 0.410(13) |
| 33.00(2) | 0.276(2) | 0.1060(8) | 0.497(13) |
| 32.00(2) | 0.263(3) | 0.182(1) | 0.79(2) |
| 31.50(2) | 0.254(8) | 0.193(3) | 1.17(7) |
| 31.00(2) | 0.251(18) | 0.408(2) | 1.44(10) |
| 30.70(2) | | 0.536(2) | |
| 30.40(2) | | 0.706(8) | |
| 30.10(2) | | 1.055(5) | |

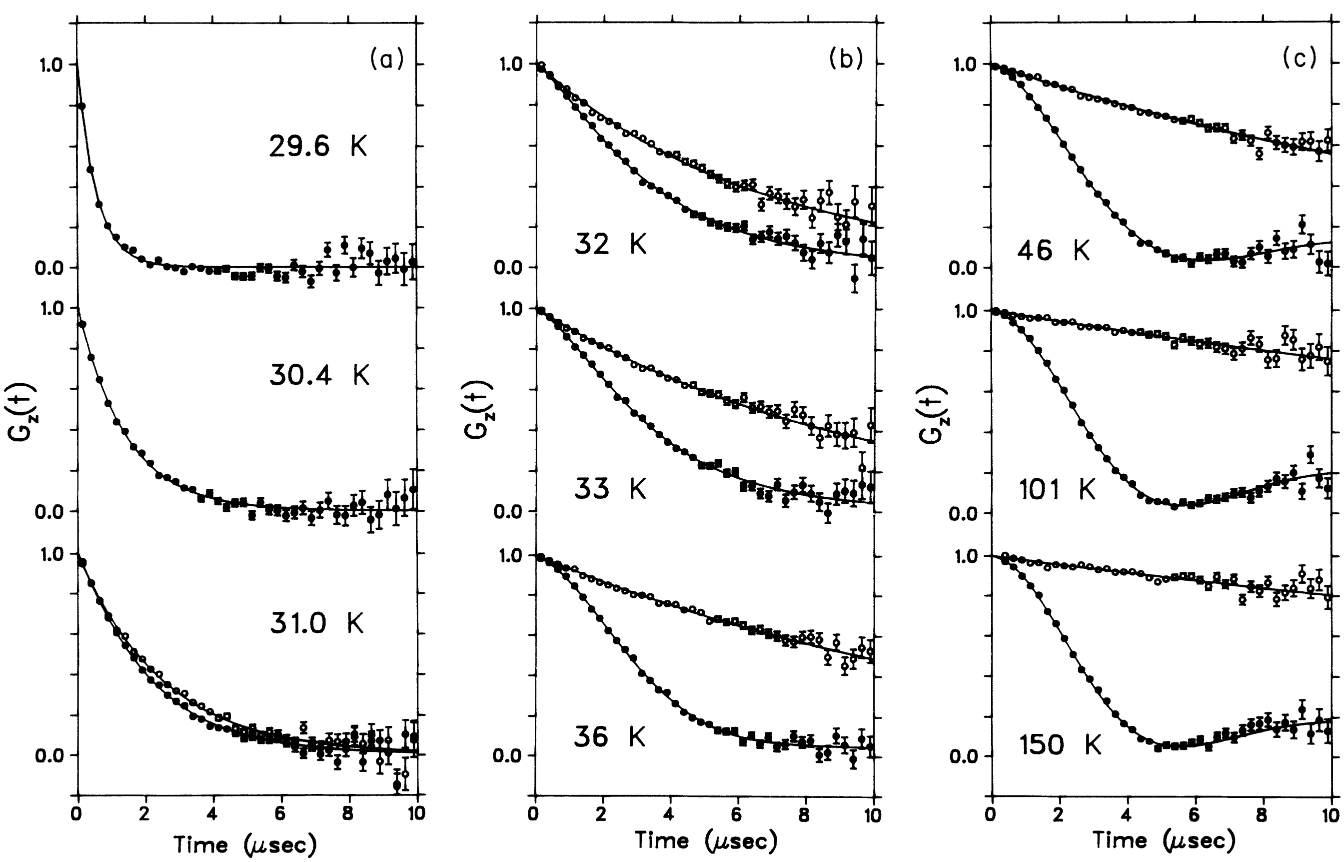


FIG. 5. Corrected asymmetry time spectra showing muon spin relaxation in the paramagnetic phase of MnSi $[G_z(t) \equiv G_{zz}(t)]$. Zero-field spectra (solid circles) and ~122-Oe longitudinal field spectra (open circles) are shown at each temperature.

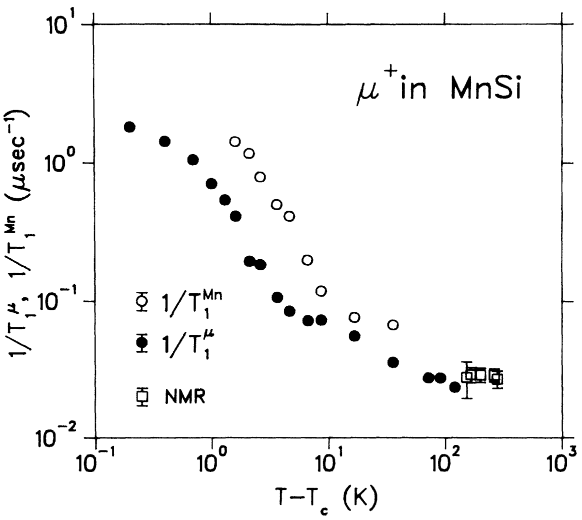


FIG. 6. Spin-lattice relaxation rate as a function of $T-T_c$ in paramagnetic MnSi. Open circles, $1/T_1^{Mn}$; solid circles, $1/T_1^{\mu}$; open squares, $1/T_1^{Mn}$ NMR data from Yasuoka *et al.* (Ref. 3).

$T-T_c$ in Fig. 8. If the $T_1$ relaxation is attributed only to the hyperfine field, the following scaling of $T_1$ is expected:

$$\frac{T_1^{\mu}}{T_1^{Mn}}=\left[\frac{\gamma_{Mn}A_{hf}^{Mn}}{\gamma_{\mu}A_{hf}^{\mu}}\right]^2 , \tag{18}$$

where $\gamma_{Mn}=2\pi\times 1.050\times 10^3$ $Oe^{-1}s^{-1}$ is the $^{55}Mn$ gyromagnetic ratio and $A_{hf}^{Mn}$ and $A_{hf}^{\mu}$ are the hyperfine fields for $^{55}Mn$ and $\mu^+$, respectively. If we use values of

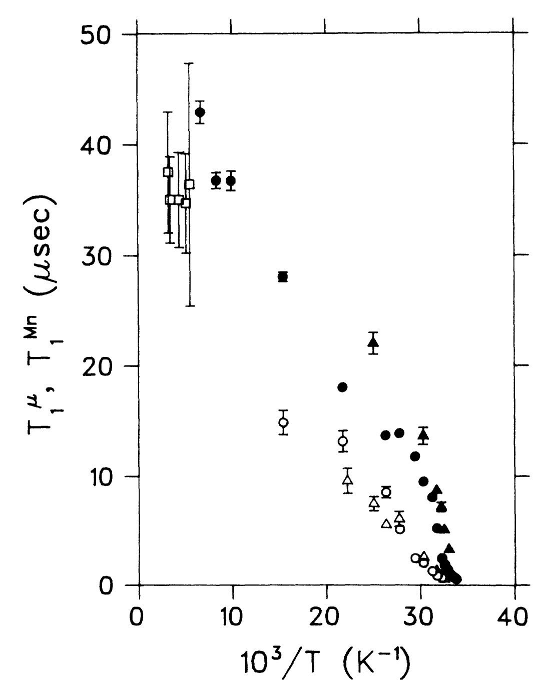


FIG. 7. Plot of spin-lattice relaxation times vs $1/T$. Open circles, $T_1^{Mn}$; solid circles, $T_1^{\mu}$; open squares, NMR $T_1^{Mn}$ data from Yasuoka *et al.* (Ref. 3). Open triangles, $T_1^{Mn}$ data from Matsuzaki *et al.* (Ref. 5); solid triangles, $T_1^{\mu}$ data from Matsuzaki *et al.* (Ref. 5).

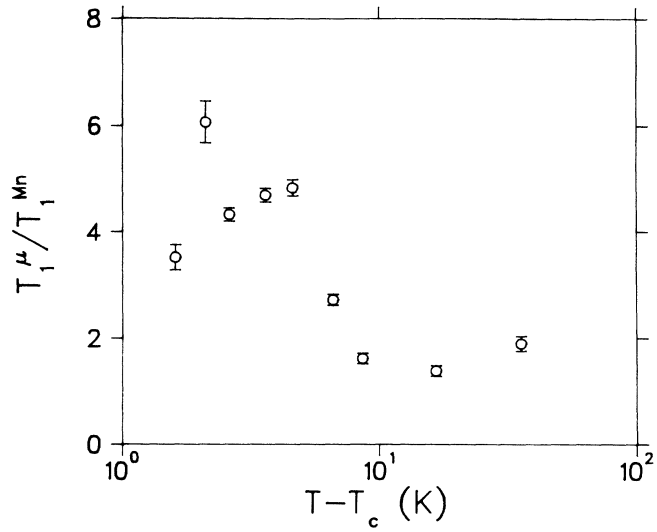


FIG. 8. Ratio of spin-lattice relaxation times $T_1^{\mu}/T_1^{Mn}$.

$A_{hf}^{Mn}=-(1.38\pm0.01)\times10^5$ $Oe/\mu_B$ (Ref. 3) and $A_{hf}^{\mu}=-(4.8\pm0.2)\times10^3$ $Oe/\mu_B$ (Ref. 14) deduced from Knight shifts in the paramagnetic phase, we obtain the ratio $T_1^{\mu}/T_1^{Mn}=5.0\pm0.3$ from Eq. (18). In the lower-temperature region ($T-T_c\leq 10$ K), this scaling factor is consistent with the present experimental value. It seems, however, that the ratio drops to 2 or less above this temperature. This suggests that the kink in $1/T_1$ versus $T-T_c$ might be related to the relative enhancement of the nuclear dipolar contribution to $G_{zz}(t)$ in this temperature range.

The fitted value of the nuclear dipolar width $\Delta$ shows a wak $T$ dependence as shown in Fig. 9. In the previous experiment the data were analyzed under the assumption that $\Delta$ is independent of temperature,[5] which was justified because of the limited temperature range. In the present analysis, however, fitting with a common average $\Delta$ yielded unacceptably poor $\chi^2$ values, especially at higher temperatures. This was the case regardless of

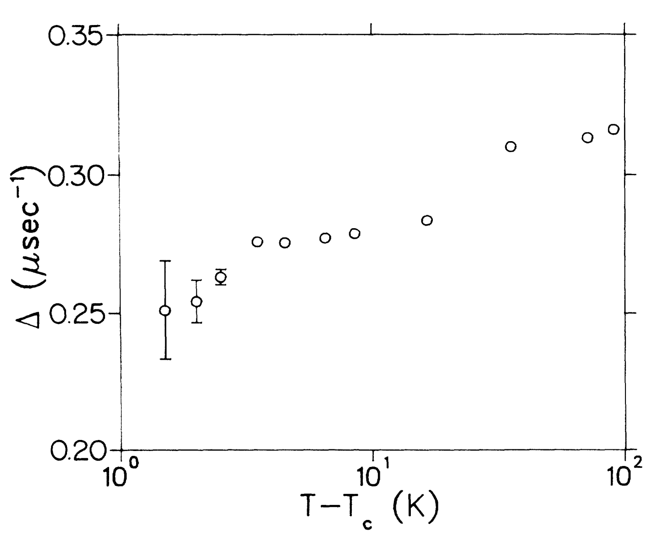


FIG. 9. Nuclear dipolar width $\Delta$ vs temperature.

whether the data were compared with Eq. (7) or Eq. (9).

Of all the physical parameters of the model, $\Delta$ seems the least likely to have any actual $T$ dependence. Most probably this discrepancy is the result of fitting to a phenomenological Gaussian Kubo-Toyabe relaxation function $G_{zz}^{\rm KT}(t;T_1^{\rm Mn})$ that is certain to be at least slightly inaccurate in the static limit. The classic example of $\mu^+$ relaxation in Cu metal[18] (with a far more symmetric muon site) was found to obey a significantly different static $G_{zz}(t)$ from that predicted by a simple Gaussian local field distribution. It would not be surprising, then, if the nuclear dipolar relaxation in MnSi were even more different from $G_{zz}^{\rm KT}$. Such a discrepancy would matter little in the limit of fast fluctuations but would distort the fitted value of $\Delta$ (and confound the effects of a long $T_1^{\mu}$ with the true shape of the static dipolar relaxation function) at temperatures well away from $T_c$. We suspect that this is the source of several of the mysterious effects observed (see above), but little can be done to alleviate this uncertainty until the muon site is determined (e.g., by LCR $\mu$SR experiments[11]) and the exact quantum-mechanical dipolar relaxation function can be calculated.[19] For the time being we must accept the apparent $T$ dependence of $\Delta$ as an empirical phenomenon.

## V. SUMMARY AND CONCLUSION

In the ordered phase of MnSi, we have shown that there are two magnetically inequivalent sites for the muon. The temperature dependences of the local magnetic field $H_{\rm loc}$ and the spin-lattice relaxation time $T_1$ have been confirmed with an improved precision compared with the previous result. The $T$ dependence of $1/T_1$ shows a deviation from the SCR prediction ($1/T_1 \propto T/M_Q^2$) for 20 K $\leq T \leq T_c$, which could be explained by the weak antiferromagnetic behavior of the helical structure.

In the paramagnetic phase the temperature dependences of $T_1^{\rm Mn}$ and $T_1^{\mu}$ are also slightly different from those predicted by the SCR theory. Each shows a $T$ dependence steeper than a Curie-Weiss-like behavior in a region $T-T_c \leq 10$ K, above which both show a weaker $T$ dependence. We would like to stress, however, that the SCR theory is still the most successful in describing the overall features of the spin-lattice relaxation time in this system. Other theories, such as Hartree-Fock calculations, could not reproduce the $T$ dependence of $T_1$ at higher temperatures. Further development of the theory is needed for a more elaborate understanding of spin fluctuations in itinerant magnets.

## ACKNOWLEDGMENTS

This work was supported by a Grant-in-Aid for the Special Project Research on Meson Science of the Ministry of Education, Science and Culture of Japan, by the Natural Sciences and Engineering Research Council of Canada and by the Canadian National Research Council.

*Present address: Metal Physics Laboratory, Institute of Physical and Chemical Research, 2-1 Hirosawa, Wako, Saitama 351-01 Japan.


[1] Y. Ishikawa, K. Tajima, D. Bloch, and M. Roth, Solid State Commun. **19**, 525 (1976).

[2] K. Motoya, H. Yasuoka, and Y. Nakamura, Solid State Commun. **19**, 529 (1976); K. Motoya, H. Yasuoka, Y. Nakamura, and J. H. Wernick, J. Phys. Soc. Jpn. **44**, 833 (1978).

[3] H. Yasuoka, V. Jaccarino, R. C. Sherwood, and J. H. Wernick, J. Phys. Soc. Jpn. **44**, 842 (1978).

[4] R. S. Hayano, Y. J. Uemura, N. Nishida, T. Yamazaki, H. Yasuoka, and Y. Ishikawa, Phys. Rev. Lett. **41**, 1743 (1978).

[5] T. Matsuzaki, K. Nishiyama, K. Nagamine, T. Yamazakie, M. Senba, J. M. Bailey, and J. H. Brewer, Phys. Lett. A **123**, 91 (1987).

[6] M. Takigawa, H. Yasuoka, Y. J. Uemura, R. S. Hayano, T. Yamazaki, and Y. Ishikawa, J. Phys. Soc. Jpn. **49**, 1760 (1980).

[7] T. Moriya and A. Kawabata, J. Phys. Soc. Jpn. **34**, 639 (1973); **35**, 669 (1973).

[8] R. S. Hayano, Y. J. Uemura, J. Imazato, N. Nishida, T. Yamazaki, and R. Kubo, Phys. Rev. B **20**, 850 (1979).

[9] Y. J. Uemura, R. S. Hayano, J. Imazato, N. Nishida, and T. Yamazaki, Solid State Commun. **31**, 731 (1979).

[10] Y. J. Uemura, K. Nishiyama, T. Yamazaki, and R. Nakai, Solid State Commun. **39**, 461 (1981).

[11] S. R. Kreitzman, J. H. Brewer, D. R. Harshman, R. Keitel, D. Ll Williams, K. M. Crowe, and E. J. Ansaldo, Phys. Rev. Lett. **56**, 181 (1986).

[12] A. Schneck, *Muon Spin Rotation Spectroscopy* (Hilger, Bristol, 1985).

[13] Y. Ishikawa, T. Komatsubara, and D. Bloch, Physica B+C **86-88**, 401 (1977).

[14] H. Yasuoka, R. S. Hayano, N. Nishida, K. Nagamine, T. Yamazaki, and Y. Ishikawa, Solid State Commun. **26**, 745 (1978).

[15] T. Moriya and K. Ueda, Solid State Commun. **15**, 169 (1974); K. Ueda and T. Moriya, J. Phys. Soc. Jpn. **38**, 32 (1975).

[16] T. Moriya, Solid State Commun. **20**, 291 (1976); K. Makoshi and T. Moriya, J. Phys. Soc. Jpn. **44**, 80 (1978).

[17] K. Makoshi, Ph.D. thesis, University of Tokyo, 1977 (unpublished).

[18] R. Kadono, J. Imazato, K. Nishiyama, K. Nagamine, T. Yamazaki, D. Richter, and J.-M. Welter, Phys. Lett. **107A**, 279 (1985).

[19] M. Celio, Phys. Rev. Lett. **56**, 2720 (1986).